

Selenium anions diffusion in bentonite in the presence of silicates

NERA RESEARCH GROUP, REACTOR INSTITUUT DELFT, TU DELFT
BSC. THESIS TUUR VERMUNT

Abstract

For safe disposal of high level nuclear waste, deep geological repositories in Boom Clay is one of the promising options in the Netherlands. Bentonite is an optional back-fill material for deep geological disposal. Selenium is one of the elements contained in the HLW and has a fission yield of only 0.04%, but due to high half-life (370000 years) and the mobility of its anions the study of selenium in safety assessment of deep geological disposal is of high importance. Silicates can be present in underground waste sites due to glass dissolution or concrete breakdown. To study the diffusion, electromigration was used to decrease experimental time. Experiments to determine the diffusion coefficients of selenite and selenate anions in bentonite, both with and without the presence of silicates, were performed. Silicate being present during the migration resulted in higher dispersion of selenate.

Selenium anions diffusion in bentonite in the presence of silicates

Tuur Vermunt
4178084

Bachelore thesis performed at:
TU Delft
Section Nuclear Energy and Radiation Applications
Radiation Science and Technology
Reactor Instituut Delft

Under supervision of:
Dr. Denis Bykov
Dr. Andrea Sabau

August 18th 2016

Table of Contents

1. Introduction	4
1.1 Geological disposal of High Level Nuclear Waste	4
1.2 Clay as backfill material	5
1.2.1 Structure	5
1.2.2 Bentonite	6
1.2.3 Diffusion through bentonite	7
1.2.4 Diffuse double layer	7
1.3 Radionuclide retention in bentonite	8
1.3.1 Selenium	8
1.4 Influence of silicate presence in bentonite on selenate retention	9
1.4.1 Silicates in bentonite	10
1.4.2 Previous research	10
1.4.3 Research questions	10
2. Experimental	11
2.1 The electromigration cell	11
2.1.1 Experimental diffusion-coefficient determination experiments	12
2.1.2 Equation for potential driven transport of particles through saturated bentonite	12
2.2 Experimental procedure	15
2.2.1 Active solution	15
2.2.2 Electrolyte water	16
2.2.3 Silicate solution	16
2.2.4 Bentonite core	16
2.2.5 Electromigration experiment	17
2.2.6 pH front experiment	18
3. Results and discussion	18
3.1 Active solution speciation	18
3.2 Electromigration experiments	19
3.2.1 $\text{Na}_2\text{SiO}_3/\text{Na}_2\text{SeO}_3$ experiments	20
3.2.2 $\text{H}_2\text{SiO}_4/\text{Na}_2\text{SeO}_3$ experiments	21
3.2.3 $\text{H}_2\text{SiO}_4/\text{H}_2\text{SeO}_4$ experiments	22
3.3 pH front experiment	26
4. Conclusions and recommendations	27
4.1 Conclusions	27
4.2 Recommendations	27
Bibliography	28
Appendices	30
Appendix 1 Matlab script used to determine apparent dispersion and velocity	30
Appendix 2 Full composition of Boom clay porewater	31
Appendix 3 LabView Script used for monitoring voltage during experiments	32

1. Introduction

1.1 Geological disposal of High Level Nuclear Waste

In the Netherlands nuclear waste is divided into three main categories; *Low- and Intermediate Level Waste* (LILW), heat generating *High Level Waste* (HLW) and non heat generating HLW. The LILW may, (i) be naturally occurring material containing large quantities of a radioactivity concentration below the exemption level and thus suitable for reuse as additives for the preparation of building materials, e.g. for road construction; or (ii) be technically enhanced naturally occurring radioactive material including, for instance, depleted Uranium originating from the Uranium enrichment facility of URENCO in Almelo and material from phosphor production. Heat generating HLW consists of the vitrified waste from the reprocessed *Spent Nuclear Fuel* (SNF) from the two nuclear reactors in Borssele and Dodewaard (closed in 1997), SNF from the research reactors in Delft and Petten, and spent uranium targets of molybdenum production. Non heat generating HLW is mainly reprocessing waste other than the vitrified residues and some decommissioning waste. Currently the HLW in the Netherlands is at interim storage for 100 years (Vardon, et al., 2012), waiting for final deep geological disposal.

In the deep geological disposal design the HLW is vitrified in a waste matrix, encapsulated and isolated by rock, salt or clay. To ensure that the HLW is completely decayed before it will be able to enter the biosphere, a five-layered barrier system is designed for rock or clay (*Figure 1*). This system consists of the engineered barriers, the nearfield, and natural barriers the far field or geosphere. All these barriers are protecting against groundwater, that could dissolve the radionuclides, from reaching the waste matrix.

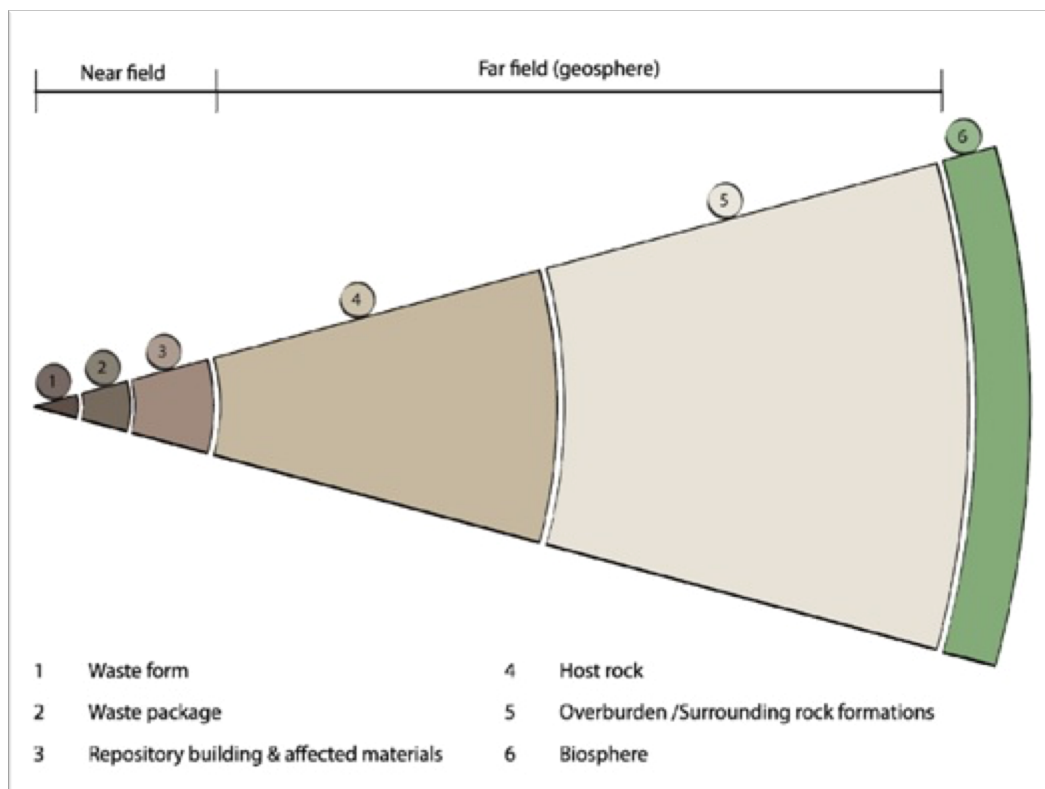


Figure 1 Schematic overview of five-layer barrier system for deep geological disposal (Verhoef, et al., 2011)

Thousands of years after the storage of the encapsulated waste, the encapsulation can break, due to: corrosion, mechanical failure or forces of nature. To stop the canister from leaking radionuclides and the leaked radionuclides, a backfill/buffer material is applied around the encapsulated waste matrix. This backfill material is also able to minimize corrosion and if needed adsorb the radionuclides (Allen & Wood, 1988). Therefore, the radionuclides are less mobile and will not be able to transport through the groundwater to the biosphere before decaying to non radiotoxic levels.

1.2 Clay as backfill material

Clay is considered as appropriate backfill material because it is a low permeable medium and has high sorption rates, which leads to high retardation of nuclides. Different saturated clay types have been researched (e.g. Bentonite and Boom Clay) (Maes, 2004). Partially-saturated systems where air and water are present are left out, due to the high pressure at the depth of possible geological disposal (300 - 500 m) no air will be present (Higgo, 1986).

1.2.1 Structure

To understand why clay minerals are a good medium for retarding radionuclides first it is important to understand the structure of clay. Clay is build from basic octahedral and tetrahedral building blocks (Figure 2). The (a) tetrahedral blocks are silicon atoms surrounded by oxygen atoms. The (b) octahedral blocks are aluminum, iron or other metallic ions surrounded by oxygen atoms. These blocks can form octahedral and tetrahedral sheets.

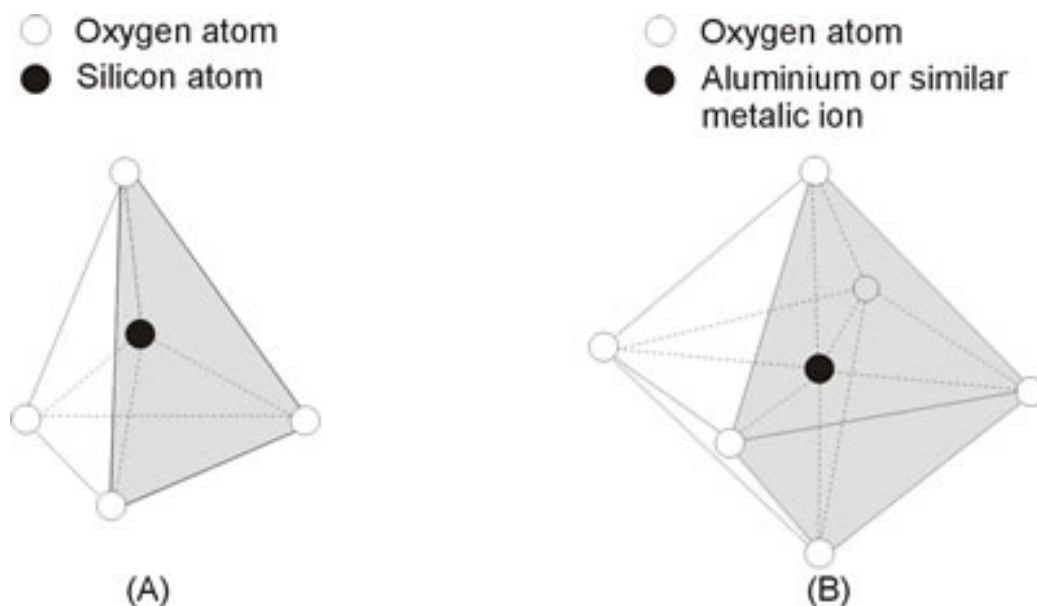


Figure 2 Schematic presentation of the building blocks for clay particles, (a) tetrahedral and (b) octahedral (Little, 1995)

Clay minerals can be classified in several groups depending on the alignment of tetrahedral to octahedral sheets and ion content. Figure 3 shows two main groups the 1:1 and 2:1, tetrahedral layers to octahedral sheets. The tetrahedral-octahedral-tetrahedral (TOT) group can again be divided in five sub-groups depending on the aqueous ion distribution between the layers.

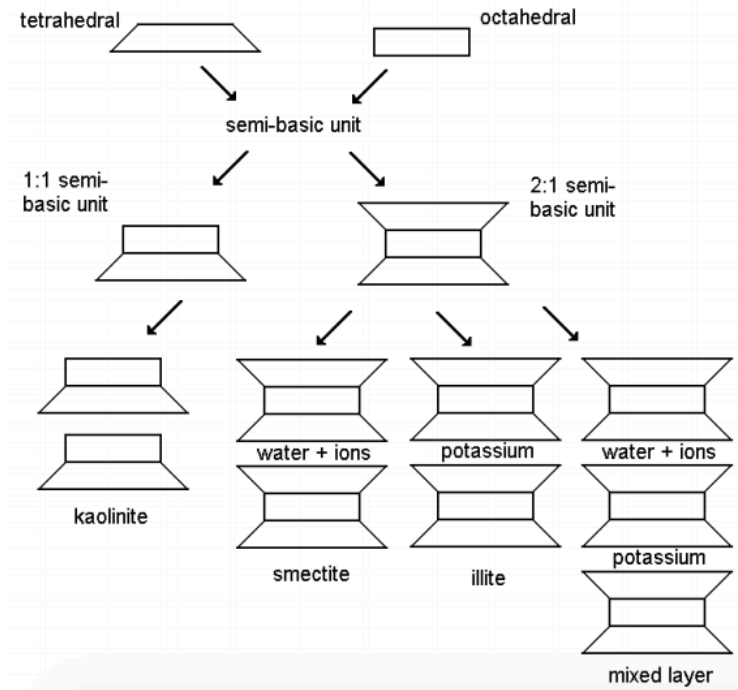


Figure 3 Different clay groups schematic presentation. (Heister, 2005)

These five groups are (i) illite have the TOT structure with interlayer potassium, (ii) smectite where the interlayers are constructed mainly by water and Na^+ and Ca^{2+} are the main interlayer cations, (iii) vermiculites are similar to smectites except with Mg^{2+} as interlayer cation. The (iv) chlorites have a TOT structure but with an octahedral sheet in the interlayer. And the (v) mixed layer is a combination of usually two 2:1 types distribution e.g. smectite-illite (Figure 3).

A set of TOT layers will form a clay particle; these clay particles will be irregular in form. Therefore, they will not be able to align properly and pores can form in the macrostructure. Through these pores dissolved ions can travel.

Clay particles in soils are always hydrated thus, surrounded by water. The properties of the clay change as the thickness of the hydration layer changes. Water is di-polar so attracted to the negative charge of the TOT layers and forms hydrogen bonds with oxygen atoms on the tetrahedral surface. Consequently, the water will be denser close to the surface and the viscosity may be 100 times higher in the first layer of water.

1.2.2 Bentonite

Bentonite is a smectite rich clay type that is considered as a backfill material for deep geological disposal of HLW (Grauer, 1994). 70% of the world bentonite is mined in Wyoming, USA. Wyoming bentonite or MX-80 is derived from volcanic ash and it contains 65–75% of Na-rich montmorillonite, 10–14% quartz, 5–9% feldspars, 2–4% mica, 3–5%

carbonates and chlorite and 1–3% heavy metals. It also has an iron content of 1-7% (IAEA, 2013) and an pH of 8.5 – 9. Wyoming bentonite (MX-80) is used in this study.

Bentonite is mainly montmorillonite as shown in Figure 4. In the structure of bentonite interlayers of water exist. The thickness of these layers is dependent on the type of cation in the water layer and the surface of the clay. If these layers get too thick radioactive isotopes would be able to transport through convection, the water flowing. In the next section will be explained that the force that drives the movement of radionuclides is caused by diffusion and not convection.

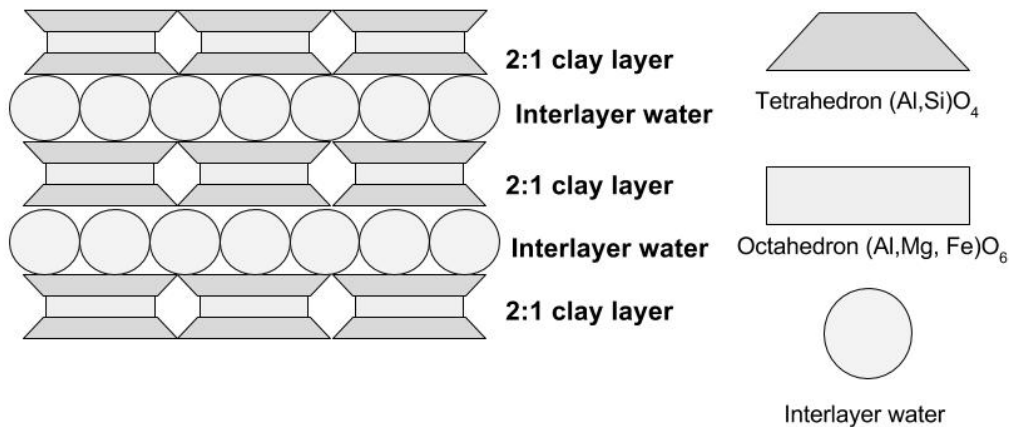


Figure 4 Schematic presentation of hydrated 2:1 clay type. The pyramids representing tetrahedrons, in the case of bentonite silicon and the blocks are octahedrons, in the case of bentonite aluminium. The round shaped interlayer objects represents water molecules with dissolved cations, in the case of bentonite mainly Na^+ and Ca^{2+} .

1.2.3 Diffusion through bentonite

The speed of transport through bentonite is almost exclusively determined by the molecular diffusion coefficient D_m [m^2/s]. It states the velocity in which the the particle will transport trough the clay. The diffusion coefficient depends on e.g. particle size, viscosity, charge and sorption capacity of the radionuclide.

Bentonite has a negatively charged surface, cations in the pore water are attracted to this charge and anions repelled. This will result in a different diffusion coefficient for these two groups. The number of cations exchangeable is the cation exchange capacity (CEC). The CEC consist of two factors: (1) The isomorphous substitution of Silica atom in the Silicate layer (octahedral) with an Aluminum atom. The negative charge created in the structure is compensated by adsorbing cations to the outer layer. These cations can be exchanged by in pore water dissolved cations. (2) The second factor being the concentration of electrolyte, which is linked to the pH of the pore water and clay surface.

The surface of bentonite is able to exchange anions on the positive edges of the Al sites. This is dependent on the electrolyte concentration and decreases with increasing pH. For pH 7 the anion exchange capacity is nearly zero. The pH of natural bentonite is between 8.5 – 9, so no anion exchange is expected. (Higgo, 1986)

1.2.4 Diffuse double layer

In aqueous environment, fine-grain clay types like bentonite, tend to form diffuse double layers. The negative surface of the clay attracts cations to compensate for the electronegativity. This results in a higher concentration of cations at the surface, further from

the surface the cations and anions are in equilibrium (Heister, 2005). The clay surface and the positively charged ions adjacent to it are called double diffuse layer is shown in Figure 5.

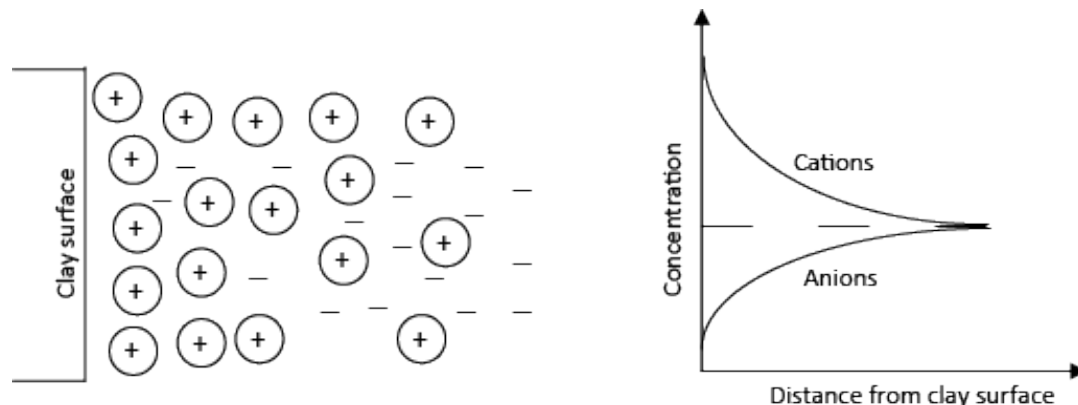


Figure 5 Schematic presentation of the diffuse watery clay-ion interface.

If in the case of aqueous compacted bentonite, the double layers of opposing layers of bentonite overlap. This will result in complete exclusion of the anions from the interlayer space in the bentonite (van Loon, et al., 2007). The anions are able to diffuse between the particles of bentonite.

1.3 Radionuclide retention in bentonite

The corrosion of the high level waste matrix leads to slow release of radionuclides into the second barrier. Backfill materials like bentonite are expected to retain these radionuclides by sorption and precipitation. The reducing environment of the bentonite create condition in which e.g. U, Pu, Np, Am and Cm are very insoluble. Therefore, these extremely toxic radionuclides would be highly immobile thus never able to reach the biosphere. The higher risk elements are less toxic but the more soluble and mobile radionuclides like ^{129}I , ^{36}Cl and ^{79}Se . (Abdelouas & Grambow, 2012)

1.3.1 Selenium

Selenium-79 is a long-lived radionuclide produced by nuclear fission products (e.g. uranium-235 and plutonium-239). ^{79}Se is a pure beta-emitter ($^{79}\text{Se} \rightarrow ^{79}\text{Br} (\text{stable}) + 1 e^{-}$, $E = 149$ keV). The latest half-life determination of selenium-79 is 377000 years (Bienvenue, et al., 2007). Although the fission yield of ^{79}Se is only 0.04% due to a long half-life and high mobility, selenium transport in bentonite is an important issue. In this study Selenium-75 is used for experiments.

Selenium is an element with great similarities to sulfur due to similar electron configuration ($1s^2 2s^2 2p^6 3s^2 3p^6 3d^{10} 4s^2 4p^4$). The possible oxidation states of selenium are -2, 0, +4 and +6, this results in different chemical species with varying mobility. Shown in the Eh-pH diagram (Figure 6) are the chemical speciation possibilities of selenium in an aquatic medium.

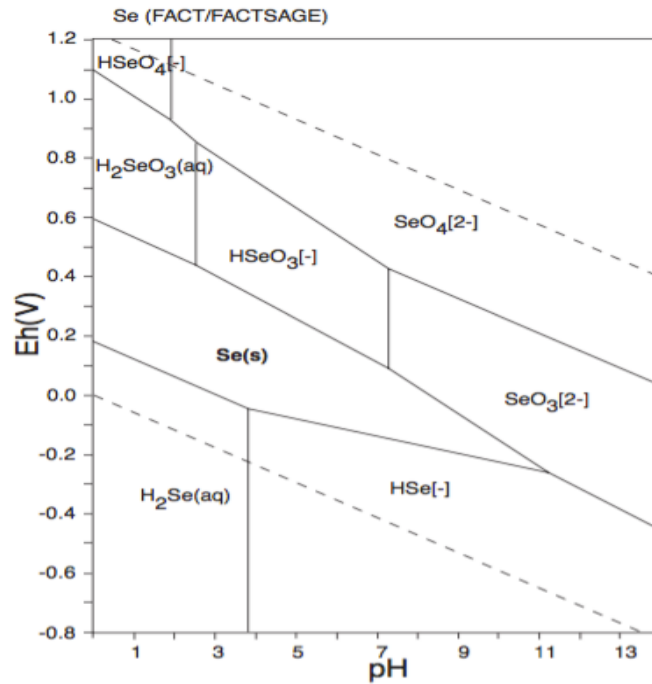


Figure 6 Eh-pH diagram of selenium in water at 298.15 K and 10^5 Pa. (Takeno, 2005)

In most aquatic ecosystems (e.g. soils, oceans) selenium occurs mostly in the +4 and +6 oxidation state, as the anions SeO_3^{2-} and SeO_4^{2-} (Duan, et al., 2010). These anions are highly mobile and therefore potentially toxic. Under bentonite conditions (pH 8-10, Eh -300mV) selenium would be expected to be mostly in the Se(-2) oxidation state in the form of HSe^- . In order to assess the in-situ speciation of selenium it is important whether redox equilibrium is achieved. Experiments in laboratory show that over a broad range of pH and Eh the species Se(+4) and Se(+6) still appear, indicating redox equilibrium is not attained (Abdelouas & Grambow, 2012). This due to slow kinetics of the selenium reduction (Foster, et al., 2003).

The speciation is important to determine the mobility of the selenium in bentonite. If all the selenium +4 (selenite) and +6 (selenate) would be reduced to immobile Se^0 or HSe^- , the ^{79}Se will not reach the ecosystem. The concentration of mobile selenite and selenate in the reducing bentonite environment will be governed by sorption-desorption. Selenite is known to form inner-sphere surface complex and selenate the weaker outer-sphere surface complex. (Snyder & Um, 2014). When selenite is sorbed to the surface a reduction-precipitation mechanism can follow, while the selenate is less likely to be sorbed nor reduced. Therefore, selenate will be the most mobile ion of selenium (Beauwens, et al., 2005).

1.4 Influence of silicate presence in bentonite on selenate retention

The complex formation of the selenium oxyanions is a big factor in the retention of the radiotoxic selenium stored in the deep geological disposal. If these complex formation site would be occupied, the diffusion rate of the selenium could be higher than modeled in selenium only experiments. The competition between anions is an effect that can be studied by comparing experiments with and without additional anion(s) introduced. Electromigration is the ideal method for testing this competition due to relative short duration of the diffusion experiments.

1.4.1 Silicates in bentonite

Silica dissolved in the aqueous phase of bentonite can possibly source from the silica in the concrete structure surrounding the bentonite backfill material. The glass waste matrix in which the HLW is vitrified will dissolve after container breach due to thousands years of corrosion or mechanical failure. This will result, if groundwater reaches the glass, in slow glass dissolution. The glass dissolution rates primarily depend on silica concentration. For the French nuclear glass R7T7 the corrosion rates are about 10^4 - 10^5 g/m²/d at 90°C (Ferrand, et al., 2006). Dissolved silica (approx. 60 mg/L) can occupy surface sites of the bentonite and prevent the selenium oxyanions from forming an inner or outer-sphere complex (Abdelouas & Grambow, 2012). Silica increasing the glass dissolution rate and having a possible competition effect on anions are the reason why it is important to study the presence of silica presence in radionuclide diffusion experiments.

1.4.2 Previous research

Electromigration experiments were previously conducted at TU Delft. Radioactive isotopes of cesium, technetium and selenium were studied separately and in competition experiments. Electromigration experiments were conducted by J. Zappey for Ce, Tc and Se in bentonite (Zappey, 2013). Resulting in one peak distribution profiles for cesium and technetium, but no distribution profile is given for selenium. During mixed experiments (Tc and Se) four overlaying distributions appeared indicating differentiating speciation or competition.

Further competition study using electromigration was done by P. Carter (Carter, 2015), studying the effect of silicate on the diffusion coefficient of selenate. The distribution profiles produced in that study had multiple peaks. No influence on the diffusion coefficient of selenate due to presence of silicate was shown in that study. However, the silicate in that study the silicate was spiked at the middle of the core in stead of saturating the whole bentonite core with silicate.

1.4.3 Research questions

In previous research the multiple peak distribution profiles remained in ⁷⁵Se experiments and in competition experiments. This effect occurred both using selenite and selenate. Experiments will be conducted to further explain these multiple peaks presented in electromigration experiment concentration profiles.

This study will focus on understanding the effect of silicate in bentonite on the retention of radionuclides. Silicates have the possibility of forming the oxyanion-surface complex therefore, competition with other anions is possible. In this study selenate retention will be studied using ⁷⁵Se and silicate saturated bentonite.

2. Experimental

2.1 The electromigration cell

The diffusion of ions through bentonite is an extremely slow process (Allen & Wood, 1988). Due to this very slow diffusion experiments, mapping out diffusion coefficients of different radiotoxic elements, will be a time-consuming task. Migration experiments can be accelerated in several ways. The most important are constructing a hydraulic pressure or an electrical field over the setup. For bentonite the permeability is very low, so the hydraulic pressure has to be extremely high. The same movement in charged species can be caused by a small electrical current. Consequently, in this study an electromigration cell is used to accelerate the diffusion process. Experimental time will be reduced from several years per experiment to 8 to 20 hours per experiment, increasing the amount of experiments done dramatically.

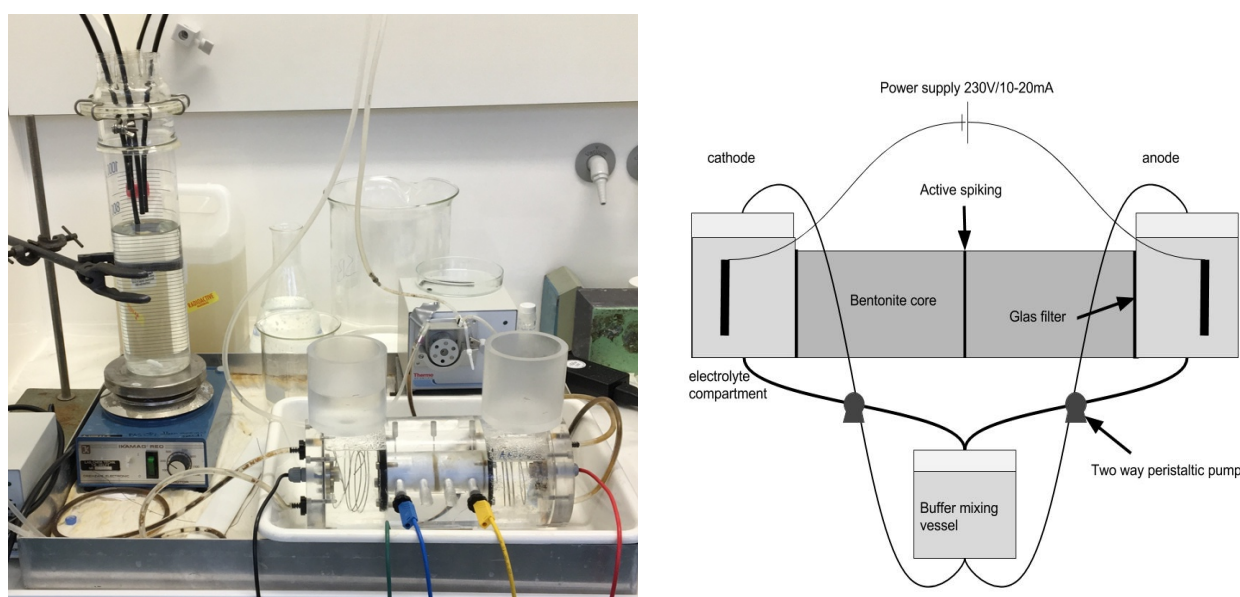


Figure 7 Picture of the electromigration set-up used in this study (left) and schematic representation of the set-up (right).

Shown in Figure 7 is the complete set-up of the electromigration cell (250 mm long). The cell consists of a 100 mm long Plexiglas core holder with an inner diameter of 30 mm. Two glass filters (VWR 511-0054) with an 40mm diameter and pore size 10-16 μm seal off the core from the electrolyte compartments (volume of 380 cm³). These filters make sure the bentonite is obstructed to diffuse into the electrolyte solution (section 2.2.2) but the electrolyte can migrate in. In the saturation process of the bentonite it is important to have the ability to retrieve the bentonite samples from the core holder while keeping them intact. Therefore, two Teflon cylindrical sample holders, 50x29.9 mm to fit to the electromigration cell perfectly are produced. The inner diameter of these sample holders are 26mm, this being the size of the sample.

The electrolyte compartments are sealed off by screwing on a lid, integrated in this lid a 1 mm thick stainless steel coil functioning as the electrode. For the experiments it was important to ensure a constant current, this was done by attaching the electrodes (red and black wire Figure 7) to an DC power supply (Aim TTi PLH250-P 250V 0,375A LXI). To measure the electric field over the core stainless steel electrode were placed in the core 12,5 mm away from the end of the core on both the anode and cathode side. The voltage was

measured (via the blue and yellow wire Figure 7) using an Agilent 34450A 5^{1/2} Digit Multimeter attached to a computer using LabView software. The LabView script used can found in appendix 3.

The catode electrolyte compartment and the anode compartment need to have the same electrolyte composition in order for the clay to have a homogeneous distribution of ions. The electrolyte compartments are sealed off by lids and in these lids two holes are drilled and tube connectors added. Via these tubes, pumps move the electrolyte solution back and forth to a 1000 cm³ mixing vessel. The peristaltic pumps (Thermo Scientific FH30) interchange the electrolyte between the compartments to the mixing vessel.

2.1.1 Experimental diffusion-coefficient determination experiments

To study the migration of radionuclides through porous media different experimental set-ups are possible. (1) Pure diffusion tests and (2) column diffusion experiments where an additional hydraulic pressure or electrical current is applied. For pure diffusion two types of experiments are possible: (i) Trough-diffusion and (ii) in-diffusion as seen in Figure 8.

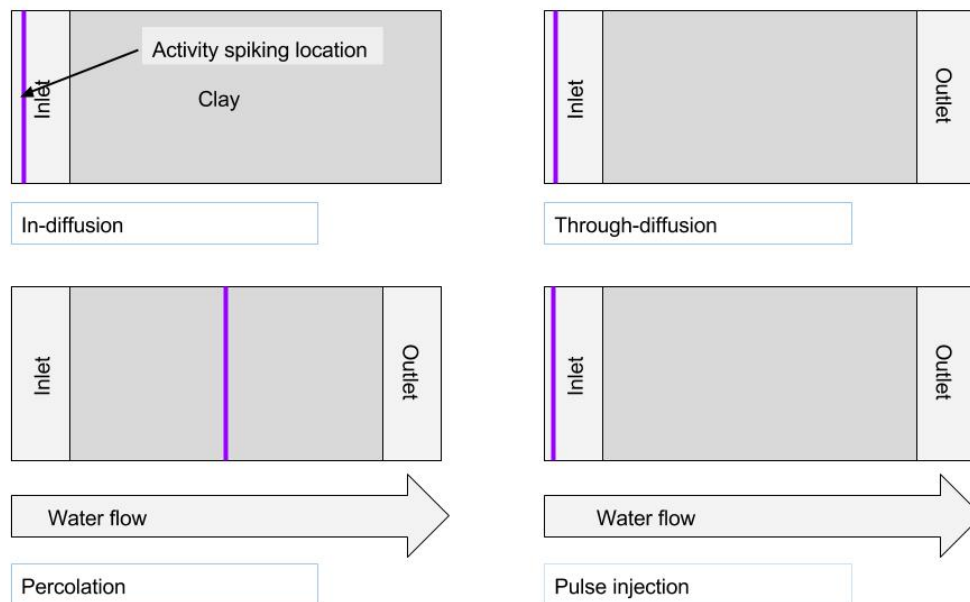


Figure 8 Schematic presentation four different types of migration experiments. Percolation and pulse injection with advection and through-diffusion and in-diffusion without advection.

Type (2) experiments, column diffusion, are shown in Figure 8 as (i) the percolation experiment and (ii) pulse injection. In pure diffusion experiments the apparent diffusion coefficient D_m^a can be measured. In experiments including advection the apparent dispersion coefficient is determined D^a (Aertesens, et al., 2008).

2.1.2 Equation for potential driven transport of particles through saturated bentonite

The potential gradient over water saturated bentonite invokes two phenomena, that are of interest for the migration of ions: (a) electromigration and (b) electroosmosis. In Figure 9 the difference is schematically presented.

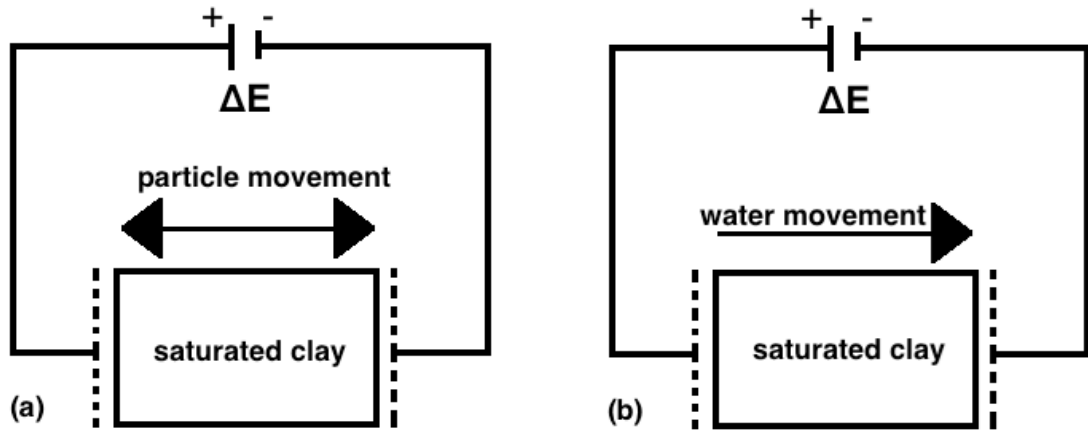


Figure 9 schematic representation of (a) electromigration and (b) electroosmosis (Heister, 2005)

Electromigration is the effect of an electrical field attracting ions towards the electrode of the opposite charge. Under influence of a potential difference an ion will obtain a certain speed described by the drift speed equation 1:

$$v = \mu E \quad (1)$$

where v is the drift speed [m/s], μ is the ionic mobility [m^2/Vs] and E is the electrical field [V/m]. The constant ionic mobility μ can be described by equation 2:

$$\mu = \frac{q}{6\pi\eta r} \quad (2)$$

where q [-] is the charge of the particle, η [Ns/m^2] is the viscosity of the medium and r [m] is the radius of the moving particle. The relationship between the molecular diffusion coefficient and the ionic mobility is given by the Einstein relation:

$$D_m = \frac{\mu K_b T}{Ze} \quad (3)$$

where D_m is the molecular diffusion coefficient [m^2/s], K_b is the Boltzmann constant, $1,38 \cdot 10^{23}$ [J/K], T is the temperature [K], Z is the valence [-] and e is the electron charge, $1,6 \cdot 10^{19}$ [C].

The transport of chemical species is a variation of Fick's second law, defined as the standard dispersion-convection equation:

$$\frac{\partial C}{\partial t} = D \frac{\partial^2 C}{\partial x^2} - V_c \frac{\partial C}{\partial x} \quad (4)$$

where the first term defines the dispersion with D [m^2/s] (dispersion coefficient) and the second term defines the convection with convection velocity V_c [m/s]. The convection velocity consists of two parts both determined by the electrical gradient:

$$V_c = v_{eo} + v_{em} \quad (5)$$

where v_{em} is the electromigration velocity and v_{eo} is the electroosmotic velocity. The electroosmotic velocity is due to electroosmosis. Electroosmosis is the result of a flow of water towards the cathode. This flow of water is resulting from the presence of an electrical double layer in the clay pores. Cations in the pore water compensate for the negatively charged surface of the clay. The cations in the double layer, under electrical current, are attracted towards the cathode, resulting in a bulk flow of pore water towards the cathode.

For a porous medium the standard dispersion-convection has to be adjusted for tortuosity and retardation. Tortuosity, τ is the ratio between the real micro-scale path length of diffusion x [m], and the macro observed path length of diffusion z [m]:

$$\tau = x/z. \quad (6)$$

The retardation factor, R is based on the assumption of isotherm linear sorption:

$$R = 1 + \frac{\rho_d K_d}{\eta_{diff}} \quad (7)$$

where ρ_d is the dry density of the clay in [kg/m³], K_d is the distribution coefficient in [m³/kg], and η_{diff} is the diffusion accessible porosity [-]. Equation 8 is an adjusted version of equation 4, $x = \tau z$ (equation 6) and correction for retardation and tortuosity are implemented:

$$\frac{\partial C}{\partial t} = \frac{D}{R\tau^2} \frac{\partial C}{\partial z^2} - \frac{V_c}{R\tau^2} \frac{\partial C}{\partial z} \quad \text{and} \quad \frac{\partial C}{\partial t} = D^a \frac{\partial C}{\partial z^2} - V_c^a \frac{\partial C}{\partial z} \quad (8)$$

where τ [-] is the tortuosity, R [-] the retardation factor, $D/R\tau^2$ the apparent dispersion coefficient D^a [m²/s] and $V_c/R\tau^2$ the apparent convection velocity V_c^a [m/s]. The superscript 'a' means: as observed in porous medium taking in to account the tortuosity and retardation. The relation between the apparent dispersion coefficient and the apparent molecular diffusion coefficient is described by equation 9:

$$D^a = D_m^a + \alpha V_c^t \quad (9)$$

with D_m^a [m²/s] being the apparent molecular diffusion coefficient and α [m] being the dispersion length. D^a is the apparent dispersion coefficient and V_c^t is the total convection velocity which differs from the apparent convection velocity V_c^a . Two different equations define V_c^t equation 10 for anions and equation 11 for cations. Figure 10 is a schematic presentation of the terms in these equations.

$$V_c^t = v_{em}^a = \frac{v_{eo}^a}{R} + V_c^a, \quad \text{in case of anions} \quad (10)$$

$$V_c^t = v_{em}^a + \frac{v_{eo}^a}{R} = V_c^a, \quad \text{in case of cations} \quad (11)$$

where v_{em}^a [m/s] is the apparent electromigration velocity and v_{eo}^a [m/s] the apparent electroosmotic velocity (Maes, et al., 1999).

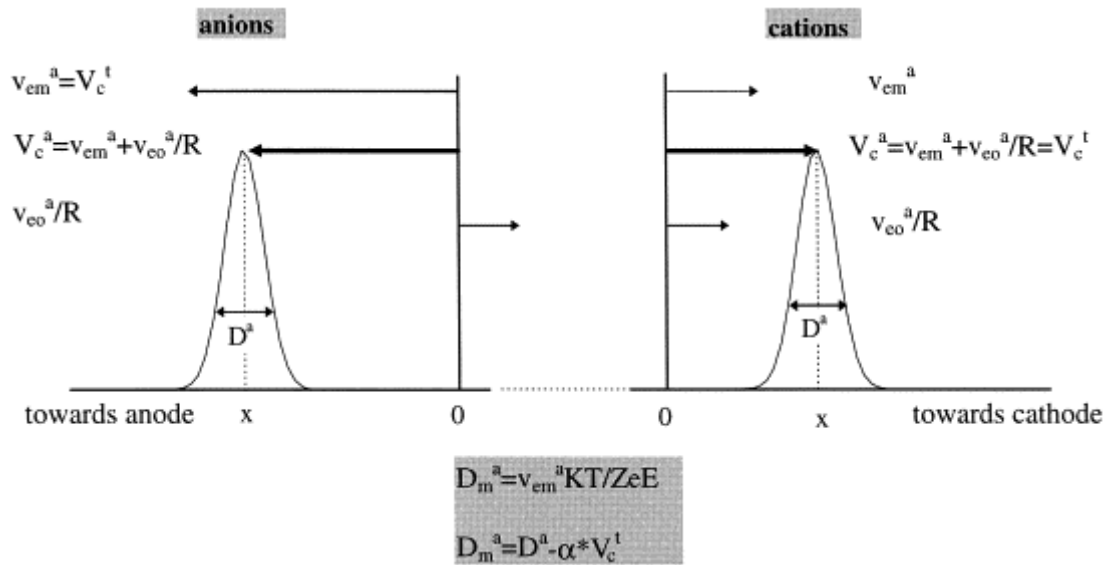


Figure 10 Representation of the electromigration experiment in terms used in equation 11 and 12. (Maes, et al., 1999)

To find the experimental dispersion coefficient the data is fitted to an analytical solution of the general dispersion-convection equation 4 using proper boundary conditions: at $x = \infty$, the concentration is 0 ($C = 0$), starting conditions are $C(0 < x < \infty, t = 0) = 0$ and $C(x = 0, t = 0) = 0$

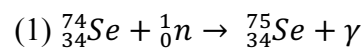
$$C(x, t) = \frac{Q_0}{2S\sqrt{\pi D^a t}} \exp\left(-\frac{(x - V_c^a t)^2}{4D^a t}\right) \quad (12)$$

where Q_0 is the initial concentration [Bq] and S is the cross-section of the clay sample [m^2]. In this thesis equation 12 is used to calculate apparent dispersion coefficients. (Maes, et al., 1999)

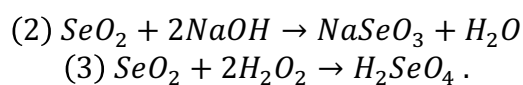
2.2 Experimental procedure

2.2.1 Active solution

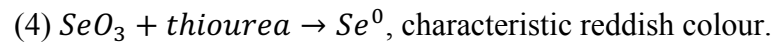
As result of the very long half-life of ^{79}Se for this experiment ^{75}Se , with a 120-day half-life was chosen to work with. To obtain a 1 MBq, 25 mg of SeO_2 was irradiated for 10 hours in the HOR reactor of the Reactor Instituut Delft. The Se was irradiated with an apithermal neutron flux of $4.45 \cdot 10^{14} \text{ s}^{-1} \text{ m}^{-2}$, a thermal neutron flux of $4.59 \cdot 10^{16} \text{ s}^{-1} \text{ m}^{-2}$ and a fast thermal flux of $3.24 \cdot 10^{15} \text{ s}^{-1} \text{ m}^{-2}$. After irradiation the sample was cooled for three days resulting in the 1 MBq of $^{75}\text{SeO}_2$. One of the neutron capture equation is given by:



The active selenium oxide sample was processed in two different ways (1) dissolved in 1ml 0.1M NaOH or (2) dissolved in 1 ml peroxide H_2O_2 . Reaction (1) produces pure selenite and (2) selenate (25g/L) (Lidin, et al., 2000):



Tests with non-active selenium are done to determine whether the above reactions are complete. To determine if selenite was present, thiourea is used to reduce selenite to elemental selenium by the reaction scheme:



Selenate is not reduced by thiourea (Waitkins & Clark, 1945).

2.2.2 Electrolyte solution

The electrolyte used in these experiments has similar chemical composition to Boom clay water. Boom clay pore water solutes consists mainly of bicarbonate (Dierkx, 1997), the full composition of BCW is presented in appendix 2. For the simplification of this study a 15 mM solution of NaHCO₃ was used as electrolyte. This solution has a pH of 8.89, close to the pH of bentonite. No pH influence would be expected.

2.2.3 Silicate solution

For the purpose of studying the competition between Se and Si anions in bentonite diffusion, a silicate solution was made close to the solubility limit to ensure any effect of silicate on selenite/selenate retention was measured. Two different sources of silicate were used in this study (1) sodium silicate (Na₂SiO₃) and (2) silicic acid hydrated (SiO₂·xH₂O, Alfa Aesar 99.99% pure). The maximum solubilities are (1) 1.8M (Alexander, et al., 1954) and (2) 0.0018M (Greenberg & Price, 1957). Which solution is used for the experiments is presented in Table 1.

Table 1 *Silicate solution used for the experiments. The solution used for experiments 1 and 2 was 25 g/L Na₂SiO₃. For experiments 3, 4 and 5 a solution of silicic acid was made in advance of clay sample preparation using 10 mg silicic acid to 100 mg of MilliQ water. Experiments 6 - 14, one solution of silicic acid hydrate was made in electrolyte water and measured by ICP to be 28.8 mg/L silicium (Optima 4300 DV, PerkinElmer instruments).*

Experiment	Silicate source used	Concentration Si (mol/L)
1 and 2	Na ₂ SiO ₃	0.2
3, 4, 5	Silicic acid hydrate	0.001
6 - 14	Silicic acid hydrate	0.001

2.2.4 Bentonite core

Proper core saturation is important for experimental determination of dispersion coefficients in bentonite. Different methods of obtaining saturated bentonite cores are discussed in previous research done by Carter (Carter, 2015). There was no difference measured between different methods therefore, the most convenient method was chosen.

For core preparation approx. 64 grams of bentonite was mixed with 100 ml of the electrolyte solution or silicate solution. This was mixed thoroughly until a homogeneous mixture was obtained; this mixture was pressed inside one of the Teflon cylinder. To ensure the cores are homogeneous a current was applied in advance of the migration experiment. In the saturation process a 15 mA current was used, the voltage was measured by LabView software. The cores were completely saturated if the potential was constant, the potential measured became constant after approximately 6 hours as seen in Figure 11.

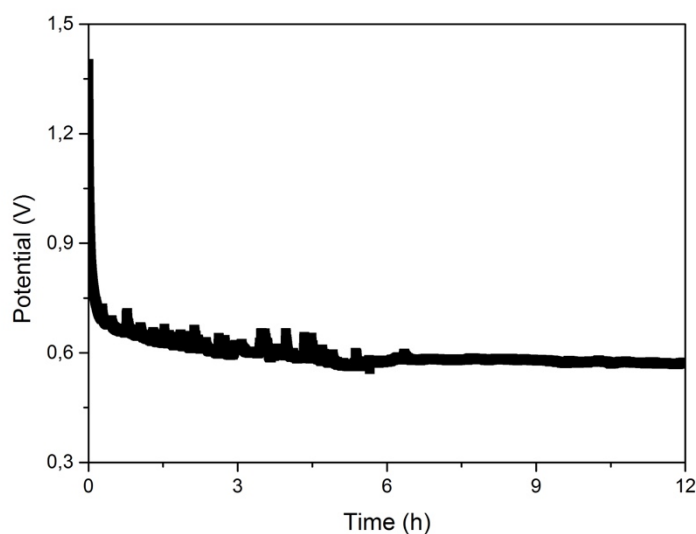


Figure 11 LabView voltage data from sample preparation.

2.2.5 Electromigration experiment

When complete saturation of the core is achieved the cell is taken apart and the two Teflon core holders containing the core are taken out of the cell. One of the two bentonite core parts is placed back, and in the middle part a piece of filter paper (\varnothing 20 mm) is placed. This filter paper is wetted with 50 μ L of electrolyte water or silicate solution, depending on the type used to prepare the clay. The wetted filter paper is spiked with 50 μ L (25g/L) of active ^{75}Se (approximately 50 kBq). The second clay core is put back in the electromigration cell and sealed off with the glass filter. The lids are screwed on and electrolyte compartments filled. Different currents were applied (10-20 mA) over the cell to perform the electromigration. During the experiment the voltage was measured using LabView and the pH was measured manually to preserve the natural pH range (8-10) for bentonite.

The electromigration experiments are in a range from 7-24 h, after the experiment the clay core is retrieved from the cell. After stopping the experiment, turning of the power, the cores were not always immediately removed from the cell. Later in this thesis this delay is referred to as a cutting delay. A Plexiglas rod (\varnothing 26 mm, (3) Figure 12) is used to push the clay out of the sample holder slowly. The bentonite cores are cut in 5 mm pieces using cutting tools ((1) and (4) Figure 12) to ensure each piece being the same thickness. The slices made are put in 50 ml plastic tubes with 40 ml MiliQ water and rotated overnight.

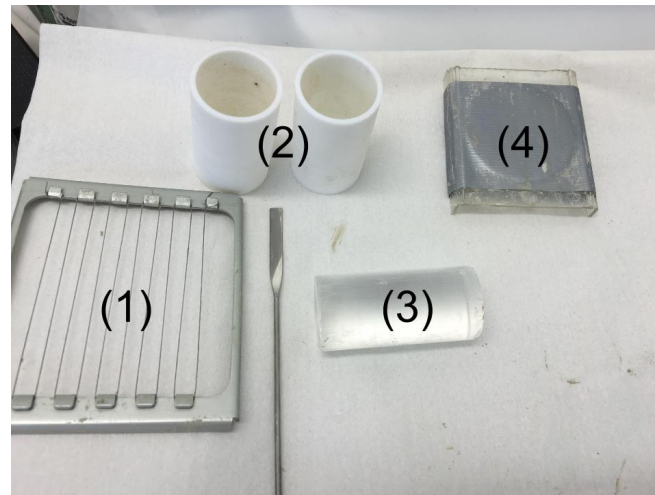


Figure 12 Photo of (1) cutting tool used, (2) sample holders, (3) the Plexiglas rod used to press out the bentonite from the sample holder and (4) the cutting plateau used.

After the samples have rotated, 10 ml was transferred to 20 ml plastic vials suitable for the Wizard 2480 automated gamma counter (Wallac). The samples were measured in the Wallac for 15 minutes, this data was extracted to excel. A Matlab script (appendix 1) was used to determine D^a and V_c^t .

2.2.6 pH front experiment

The scope of the pH front experiment was to find if pH differences occur within different parts of the clay core as a result of conducting the electromigration experiment, because the pH is an important factor in speciation. This is done by conducting an electromigration experiment without mixing the electrolyte compartments and without spiking the middle. The 15 mA current was applied for 4 hours thereafter the clay was processed in the same manner. The samples were rotated overnight and then the pH was measured using a Metrohm 744 pH meter.

3. Results and discussion

3.1 Active solution speciation

In previous research (Carter, 2015) (Zappey, 2013) it was shown that some of the distribution profiles of selenite have multiple peaks. Due to these multiple peaks the dispersion and velocity of the selenite were hard to obtain. Several explanations are possible: (1) redox reactions during the electromigration process, (2) sorption-desorption reactions, (3) initial solution already contained a mixture of oxidation states. To exclude the possibility of (3) experiments using thiourea were done to provide knowledge about the oxidation state of the

selenium (4+ or 6+). The active solutions were either prepared by dissolving the irradiated SeO₂ in 1 mL of 30% H₂O₂ or 0.1M NaOH solution as discussed in chapter 2.2.1. The experiments were done without activity but in the same ratio as the initial active solution preparation (25mg SeO₂ to 1 ml solution). Table 2 shows the results of the experiments which were performed using thiourea.

Table 2 Results of experiments performed using thiourea to determine the presence of SeO₃²⁻ in the active samples. The experiments are with non-active selenium oxide and using the same ratio as in active sample preparation. Experiments names indicate the solution used to dissolve the selenium oxide.

Name	SeO ₂ (mg)	Time before red precipitation appeared (h)
H ₂ O ₂ -1	24.8	-
H ₂ O ₂ -2	32.0	-
NaOH-1	25.0	16
NaOH-2	25.8	instantaneously
NaOH-3	25.5	instantaneously
NaOH-4	27.7	16
NaOH-5	28.0	instantaneously

The results show that the samples prepared by the dissolution of SeO₂ in H₂O₂ no precipitation occurs indicating the absence of SeO₃²⁻ in the solution. Samples prepared using a NaOH solution instead of H₂O₂ show either instant red precipitation or after one day. The difference in the five duplicates of the same experiment are possibly due to slow dissolution of selenium dioxide in the NaOH solution (Clark & Waitkins, 1945), the thiourea could have been added before the SeO₂ dissolved. The SeO₂ itself does not react with thiourea to elemental selenium (Clark & Waitkins, 1945). The thiourea was added after the NaOH solution but this was not timed. The speciation of selenium in the solution prepared by dissolving the SeO₂ in 0.1M NaOH solution could not be properly determined.

3.2 Electromigration experiments

Different electromigration experiments were conducted, as discussed in chapter 2.2.3. The data collected was all processed in a similar way, by plotting the normalized activity (activity [Bq] measured divided by the sum of all activities measured) vs. the place (distance from spiking the active solution). The graphs are labeled with the experiment number and current applied for which duration. Equation 12 is fitted to the experimentally found activity profile to find the appropriate dispersion coefficient.

3.2.1 Na₂SiO₃/Na₂SeO₃ experiments

Experiments one and two are performed by saturating the bentonite core with a sodium silicate solution (0.2M). An active selenite (selenium 4+) solution was used and activity profiles obtained are shown in Figure 13.

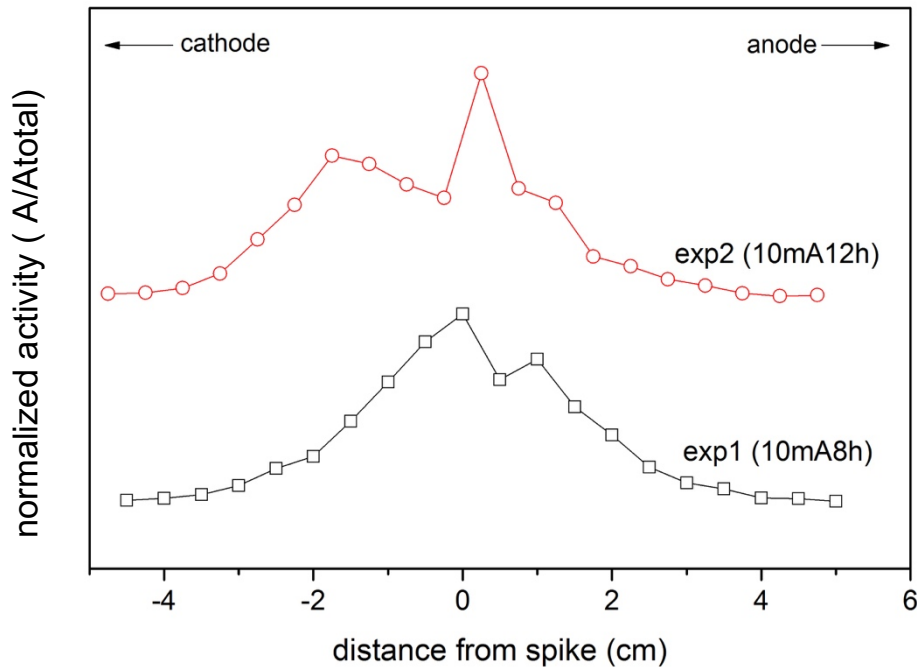


Figure 13 Concentration profiles of selenite in experiment 1 and 2. The bentonite cores were prepared using a 25g/L Na₂SiO₃ solution.

The values of V_c^a found using Matlab, are not as expected and for experiment 1 even negative as shown in Table 3. This is negative value can be caused by low duration and the first two peaks did not split but become one negative peak just in front of the zero point. The apparent dispersion coefficients are in the same region as in previous research (Zappey, 2013).

Table 3 Experiment 1 and 2 specifications and results.

Name	Duration (h)	Current (mA)	V_c^a (m/s)	D^a (m ² /s)
Exp1	8	10	-1.74E-08	2.92E-09
Exp2	12	10	5.79E-08	1.55E-09

The activity profiles consist of multiple peaks and this is explained in previous research (Carter, 2015) as different species of selenium. Three peaks are visible in experiment 2 (-1.75, 0.25 and 0.75) indicating the same results as previous research shows in Figure 14. The incomplete oxidation selenium oxide causes the multiple peaks according to other experiments done with selenite (Beauwens, et al., 2005). The retention of selenite is explained by the formation of ternary complexes with Ca or precipitation of calcium selenites (Hofmanova, et al., 2012).

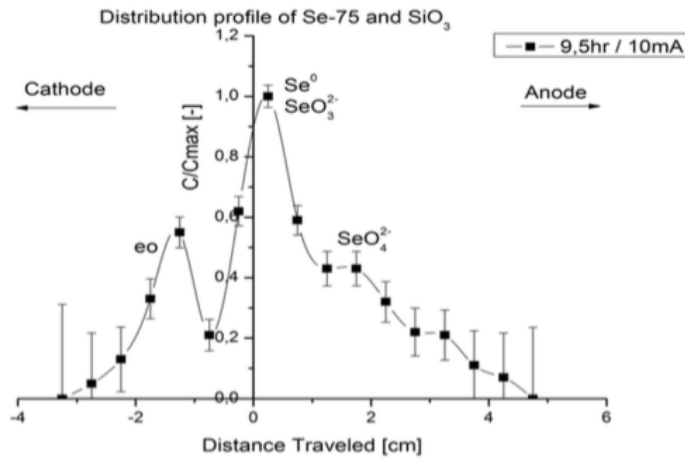


Figure 14 Activity profile found in the research of Carter. Showing three labeled peaks, an electro osmosis, selenite/selenium and selenate peak (Carter, 2015). These experiments were performed using a selenite solution and a metasilicate solution of 2×10^{-5} mol/L.

The bentonite cores prepared with the Na_2SiO_3 needed more bentonite powder to get the same consistency as with normal electrolyte solution (15mM NaHCO_3), possibly as a result of the high pH (12-13) of the sodium silicate solution. This is why following experiments were done with silicic acid.

3.2.2 $\text{H}_2\text{SiO}_4/\text{Na}_2\text{SeO}_3$ experiments

Experiments 3, 4 and 5 are done by saturating the bentonite core with a silicic acid hydrate solution (pH 8-9). The same active selenite solution was used as in experiments 1 and 2. Figure 15 shows the concentration profiles obtained.

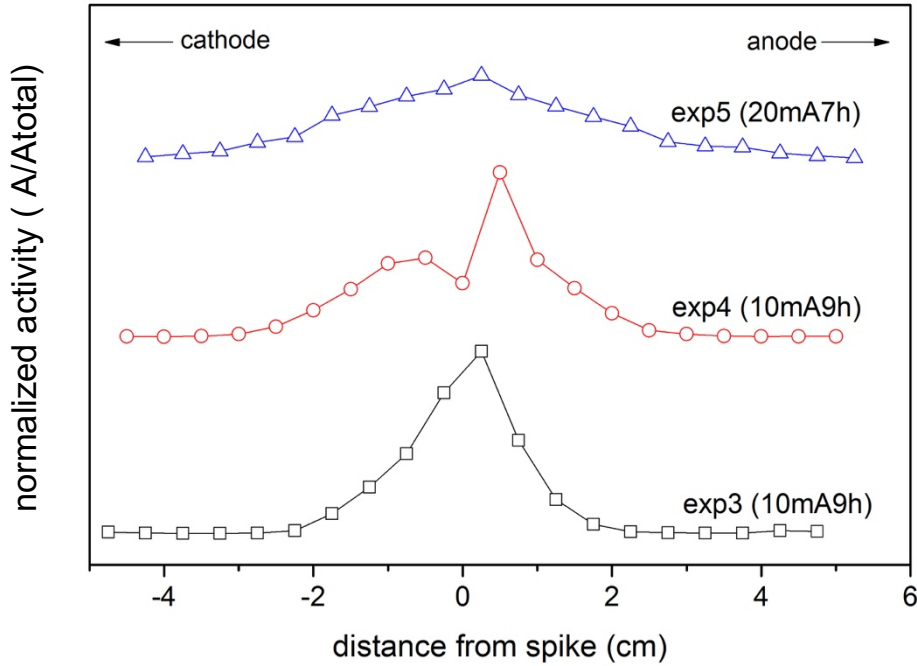


Figure 15 Concentration profiles of selenite in experiments 3,4 and 5. The bentonite cores were prepared using 100mg/L $\text{SiO}_2 \cdot x\text{H}_2\text{O}$.

The activity profiles show multiple peaks which can be the result of a redox process during electromigration. The peak towards the cathode can be caused by electroosmotic drag (Carter, 2015). Table 4 displays that the dispersion (broadness of peaks) is not solely dependent on increasing V_c^a , experiment 5 the lowest velocity and the highest dispersion was measured. The dispersion coefficients found are in the range (10^{-10}) as expected based on previous research (Beauwens, et al., 2005).

Table 4 Experiments 3,4 and 5 specifications and results.

Name	Duration (h)	Current (mA)	V_c^a (m/s)	D^a (m^2/s)
Exp3	9	10	7.72E-08	6.41E-10
Exp4	9	10	1.39E-07	6.81E-10
Exp5	7	20	2.98E-09	4.54E-09

3.2.3 $\text{H}_2\text{SiO}_4/\text{H}_2\text{SeO}_4$ experiments

Experiments 6-13 are done using selenate instead of selenite to overcome multiple peak activity profiles, thus being able to determine the effect of silicate with more accuracy. These experiments are done by saturating the clay either with the 15mM NaHCO_3 solution or with silicic acid solution (28 mg/L, silicium). The concentration profiles were created by tracing the selenate in the bentonite. The resulting distributions are shown in Figure 16 and Figure 17. Experiments 6-9 are performed without silicate to form a baseline for the determination of a diffusion coefficient for selenate in bentonite. Experiments 10-13 are performed to experimentally determine the effect of silicate on selenate retention.

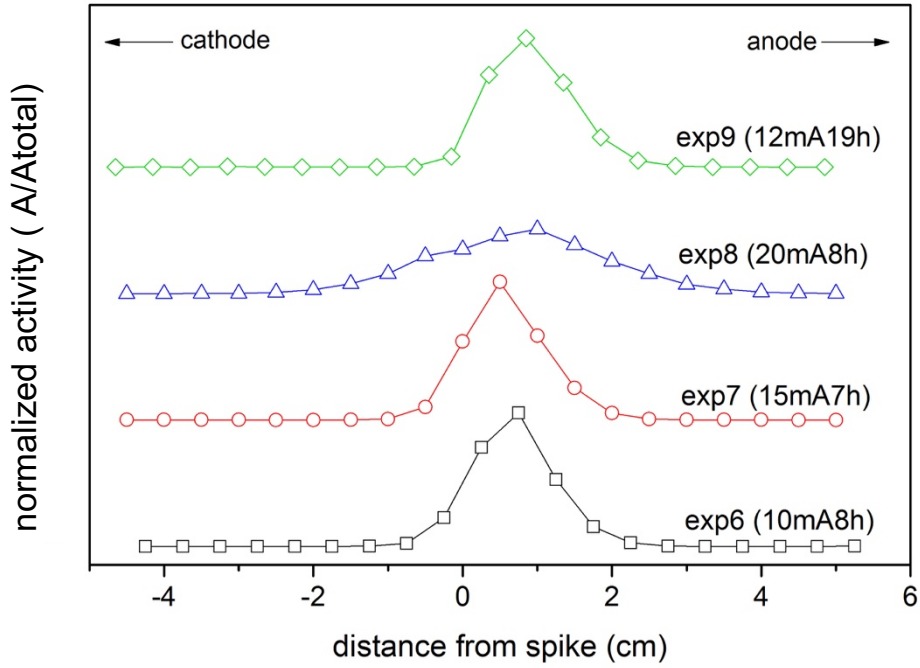


Figure 16 Activity profiles of selenate experiment 6,7,8 and 9. The bentonite cores are prepared using pure SBCW and no silicate. The distributions showed no shoulders near the peaks and clear movement of the selenate towards the anode.

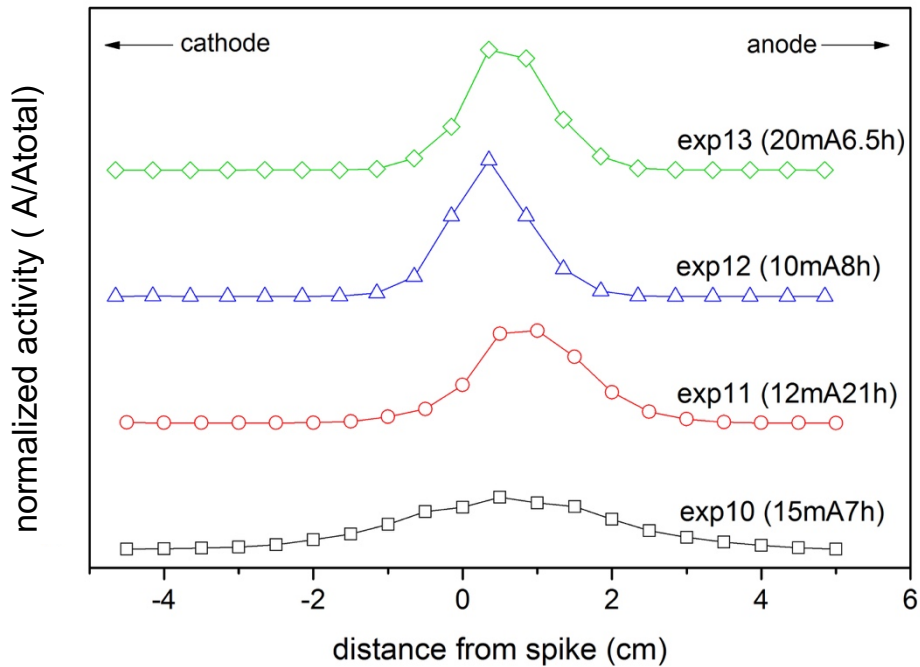


Figure 17 Activity profiles of selenate experiment 10, 11, 12 and 13. The bentonite cores are prepared using silic acid solution (0.001M Si). The distributions showed no shoulders near the peaks and clear movement of the selenate towards the anode.

Table 5 Results and specifications of experiments 6 up till 13.

Current (mA)	Name	Silicate yes/no	Duration (h)	V_c^a (m/s)	D^a (m²/s)	Cutting delay (h)
10	Exp6	no	8	1,74E-07	5,12E-10	16
10	Exp12	yes	8	1,39E-07	4,97E-10	16
12	Exp9	no	19	1,24E-07	2,16E-10	0
12	Exp11	yes	21	1,32E-07	3,73E-10	0
15	Exp7	no	7	1,98E-07	5,50E-10	16
15	Exp10	yes	7	1,98E-07	4,15E-09	88
15	Redo Exp10	yes	7	9,92E-08	2,59E-09	88
20	Exp8	no	8	3,42E-07	2,53E-09	64
20	Exp13	yes	6,5	1,50E-07	8,14E-10	16

The peaks in Figure 16 and Figure 17 have no shoulders and the activity peak moved towards the anode as a result of the electric field applied. These Gaussian-shaped distributions are comparable to activity plots obtained in electromigration experiments performed with SeO_4^{2-} (aq) in previous research (Beauwens, et al., 2005).

Table 5 shows experiment 8 and 10 have considerably broader peaks, thus having an outlying dispersion coefficient. One possible common variable that might have caused this broader peaks is the higher cutting delay than all other experiments. The cutting delay being, the time between the end of the experiment and the removal of the cores from the electromigration cell followed by cutting the clay. Experiment 10 is repeated and a same outlying result is obtained. These results indicate that the cutting delay has an effect on the dispersion of the selenate. The experiments with extremely high cutting delay have an apparent dispersion coefficient 10 times higher than no or low cutting delay experiments.

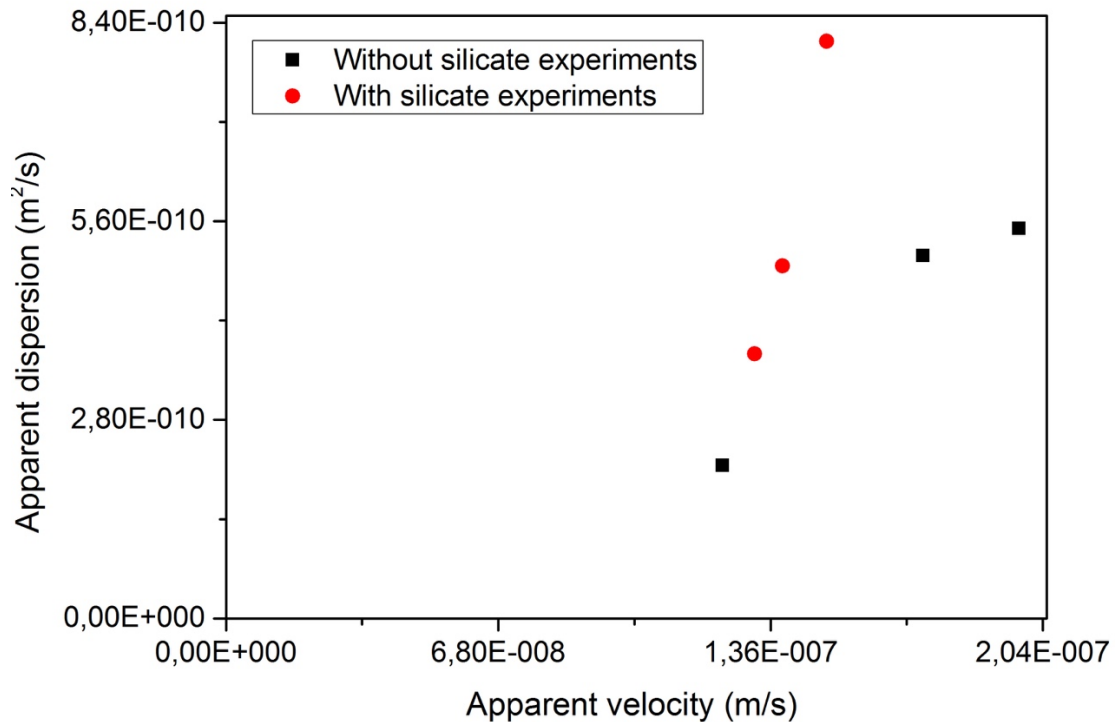


Figure 18 Apparent velocity (m/s) plotted vs. apparent dispersion (m²/s)

To determine a apparent diffusion coefficient of selenate with and without silicate a plot has been made of V_c^a vs. D^a for experiments 6, 7, 9, 11, 12, and 13 (Figure 18). The outlying results of experiment 8 and 10 are left out of this graph for reasons explained in last paragraph. In this figure if the points are extrapolated and the intersection with y-axis is taken as the apparent diffusion coefficient. This value would be negative in both cases, silicate and non silicate experiments.

It is likely this negative value might be caused by the fact that the variation of current and time is not large enough to ensure a reliable extrapolation of the line. In other research (Beauwens, et al., 2005) more points are taken to result in a positive diffusion coefficient.

All experiments involving silicate give higher dispersion coefficients of selenate in bentonite than the same experiment without silicate, implying an effect of silicate being present on the dispersion of selenate in bentonite. Silicate has a apparent diffusion coefficient of 10^{-11} (Curti, 1993), this high retardation occurs through sorption (De Cannière, et al., 1998). This sorption can have an effect on the retardation of selenate which has the ability to form inner sphere complexes with alumina sites (Loffredoa, et al., 2011).

3.3 pH front experiment

As shown in Figure 19 the pH through the clay remained constant. The experiment was not run as long as an active experiment, but the high pH change in the electrolyte compartment could have caused damage to the electrode. Due to no mixing a pH gradient set from anode to cathode electrolyte compartment, pH 9.8 for cathode and 6.7 for anode. This pH gradient is significantly higher than measured for active experiments with mixing (pH 8.5-9.0). In previous research (Zappey, 2013) also had values for pH 10 for the cathode and 6 for the anode.

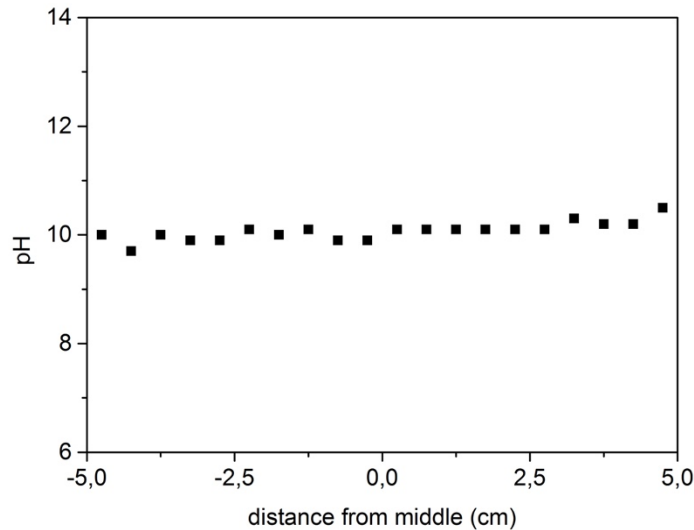


Figure 19 pH measured from cathode (-5) to anode (+5).

The experiment is done without repetition. There is no pH front measured or any pH difference through the core. The experimental time was shorter but if a pH front would exist it should have shown in this experiment without mixing. Thus, the pH change during the experiment can be excluded as a possible reason for the appearance of several peaks, observed in the case of selenite experiments.

4. Conclusions and recommendations

4.1 Conclusions

Experiments have been performed to determine the oxidation state of selenium in the active samples, therefore determining whether selenite or selenate was the main anionic form of selenium. When prepared using a NaOH-solution (0.1M), selenium was present as selenite. When prepared using H₂O₂ (30%) the absence of selenite was proven, these samples contained solely selenium as selenate.

The combined selenite/silicate experiments resulted, as in previous research (Carter, 2015), in multiple peak activity distributions. However, the selenate/silicate experiments resulted in clear one peak distribution profiles. To determine if a differentiating pH in various parts of the clay was a factor to enable oxidation or reduction of the selenite, a pH front experiment was done. The results show that the pH remains constant throughout the whole bentonite core, during the experiment.

Eight experiments were done using selenate, both with and without the presence of silicate, the dispersion versus velocity plot extrapolation, resulted in negative diffusion coefficients. Low variety in experimental time and current can be an explanation of these unexpected diffusion coefficients. Experiments performed with a bentonite core prepared using silicate solution resulted in higher apparent dispersion coefficients.

4.2 Recommendations

Experiments done indicate an effect of silicate on the retention of selenate in bentonite however this effect is marginal and no diffusion coefficient could be determined. To determine a diffusion coefficient for selenate more experiments need to be performed with a higher variety in experimental duration and current. This has to be repeated for experiment performed including silicates to obtain a conclusion about the effect of silicate on the retention of selenate.

Experimentally determining distribution of selenite in bentonite using the electromigration cell did not succeed. Multiple peaks appeared on the experimental curve while according to literature only the selenite form should be present in the sodium hydroxide prepared selenium dioxide. So the potential applied during the experiment can be the cause of these multiple peaks. The oxidation state of Se in the selenite experiments is yet unknown and need to be further researched, possibly using XAS spectroscopy.

Delay between cutting the bentonite core and stopping the experiments has an effect on the dispersion measured. Future research should take this in to account when determining dispersion using the electromigration cell.

Bibliography

- Abdelouas, A. & Grambow, B., 2012. Aquatic chemistry of long-lived mobile fission and activation products in the context of deep geological disposal.
- Aertesens, M. et al., 2008. Overview and consistency of migration experiments in clay. *Physics and Chemistry of the Earth*, pp. 1019-1025.
- Aertesens, M., De Cannière, P. & Moors, H., 2003. Modelling of silica diffusion experiments with ^{32}Si in Boom Clay. *Journal of Contaminant Hydrology*, Volume 61, pp. 117-129.
- Alexander, B., Heston, W. & Iler, R., 1954. Solubility of amorphous silica in water. *Physical Chemistry*, pp. 453-455.
- Allen, C. C. & Wood, M. I., 1988. Bentonite in nuclear waste disposal: A review of research in support of the basalt waste isolation project. Applied clay science. *Applied clay science*, Volume 3, pp. 11-30..
- Argyris, P., Chumak, A. A., Maragakis, M. & N., T., 2009. Negative diffusion coefficient in a two-dimensional lattice-gas system with attractive nearest-neighbor interactions. *Physical Review B*, p. 80.
- Beauwens, T. et al., 2005. Studying the migration behaviour of selenate in Boom clay by electromigration. *Engineering Geology*, pp. 285-293.
- Bienvenue, P., Cassette, P. & Adreolletti, G., 2007. A new determination of ^{79}Se half-life. *Applied Radiation and Isotopes*, pp. 355-364.
- Carter, P., 2015. *The influence of competition between selenate en metasilicate ions on their behaviour in bentonite*, Delft: TU Delft.
- Clark, G. R. & Waitkins, C. W., 1945. Selenium Dioxide: Preparation, Properties, and Use as Oxidizing Agent.. *Chemical Reviews*, pp. 235-289.
- Curti, E., 1993. *Modeling bentonite pore waters for Swiss high-level nuclear waste repository*, Worenlingen and Villigen: NAGRA.
- De Cannière, P. et al., 2010. *Behaviour of selenium in Boom Clay*, Mol: SCK*CEN.
- De Cannière, P. et al., 1998. Diffusion and Sorption of ^{32}Si -labelled Silica in the Boom Clay. *Radiochimica Acta*, 82(1), pp. 191-196.
- Dierckx, A., 1997. *Boom clay in situ porewater chemistry*, Mol: SCK-CEN.
- Duan, L. et al., 2010. Distribution of selenium and its relationship to the eco-environment in Bohai Bay seawater. *Marine Chemistry*, pp. 87-99.
- Ferrand, K., Abdelouas, A. & Grambow, B., 2006. Water diffusion in the simulated French nuclear waste glass SON 68 contacting silica rich solutions: Experimental and modeling. *Journal of Nuclear Materials*, pp. 54-67.
- Foster, A., Brown, G. & Parks, G., 2003. X-ray absorption fine structure study of As(V) and Se(IV) sorption complexes on hydrous Mn oxides. *Geochimica et cosmochimica acta*, pp. 1937-1953.
- Greenberg, S. A. & Price, E. W., 1957. The solubility of silica in solutions of electrolytes. 61(11), pp. 1539-1541.
- Heister, K., 2005. *Coupled transport in clayey materials with emphasis on induced electrokinetic phenomena*, Utrecht: University of Utrecht.
- Higgo, J., 1986. Clay as a barrier to radionuclide migration. *Progress in Nuclear Energy*, 5 June, pp. 173-207.

Hofmanova, E., Volka, K., Brynych, V. & Vopalka, D., 2012. Study of retention mechanism of selenite on Ca/Mg bentonite. In: *Clays in natural and engineered barriers for radioactive waste confinement - 5 International meeting Book of abstracts*. s.l.:s.n., p. 923.

IAEA, 2013. *Characterization of Swelling Clays as Components of the Engineered Barrier System for Geological Repositories*, Vienna: IAEA.

Lidin, R., Andreeva, L. & Molochko, V., 2000. Chemical properties of inorganic compounds. In: s.l.:Moscow Chemistry, p. 480.

Little, D. N., 1995. *Fundamentals of the Stabilization of Soils With Lime*. Texas: Texas A&M University.

Loffredoa, N., Mounierb, S., Thiry, Y. & Coppina, F., 2011. Sorption of selenate on soils and pure phases: kinetic parameters and stabilisation. *Journal of Environmental Radioactivity*, 102(9), pp. 843-851.

Maes, N. et al., 1999. The assesment of electromigration as a new technique to study diffusion of radionuclides in clayey soils. *Journal of Contaminant Hydrology*, pp. 231-247.

Maes, N. et al., 1999. The assesment of electromigration as a new technique to study diffusion of radionuclides in clayey soils. *Journal of Contaminant Hydrology*, pp. 231-247.

Snyder, M. & Um, W., 2014. dsorption Mechanisms and Transport Behavior between Selenate and Selenite on Different Sorbents. *Int J Waste Resources*.

Takeno, N., 2005. *Atlas of Eh-pH diagrams*, Japan: National Institute of Advanced Industrial Science and Technology.

van Loon, M., Glaus, W. & Muller, S., 2007. Anion exclusion effects in compacted bentonites: Towards a better understanding of anion diffusion. *Applied geochemistry*, pp. 2536-2552.

Vardon, P., Hicks, M., Fokker, P. & Fokkens, J., 2012. *Technical feasibility of a concept radioactive waste disposal facility in boom clay in the Netherlands*. Montpellier, s.n.

Verhoef, E., Neeft, E., Grupa, J. & Poley, A., 2014. *Outline of a disposal concept in clay*, s.l.: s.n.

Yu, J. & Neretnieks, I., 1997. *Diffusion and sorption properties of radionuclides in compacted bentonite*, Stockholm: Swedish nuclear fuel and waste management company.

Zappey, J., 2013. *Radionuclide migration in the nearfield of geological respository*, Delft: TU Delft.

Appendices

Appendix 1 Matlab script used to determine apparent dispersion and velocity

```
close all;
clc;
clear;

%import activity data from excell
ActivityData = xlsread('ActivityInputExp5');
xSpike = ActivityData(1,6);
xData = ActivityData(1:20,1) - xSpike;
cData = ActivityData(1:20,3);
radius = ActivityData(1,5)*0.01;

%process data to calculate Dapp and Vapp
x = xData.*0.01; %distance in meters
Atot = ActivityData(21,2)/900; %total activity in Bq
s=(radius^2)*0.25*pi; %surface of slice
t = ActivityData(1,4)*3600; %time in seconds

%calculate Vtot
xmax = find(cData == max(cData));
Vtot = (xData(xmax)*0.01)/t;

DmStap = 1e-13;
[Dm] = 1e-12;
[E] = 100;
for i = (2:1e5);
    Dm(i) = Dm(i-1) + DmStap;
end

for i = (1:1e5);
    c_calc1 = (Atot./(2.*s.*sqrt(pi.*Dm(i)*t))).*exp(-((x-Vtot.*t).^2)/(4.*Dm(i)*t));

    c_calcTot = sum(c_calc1);
    c_calc = c_calc1/c_calcTot;

    E(i) = sum((c_calc-cData).^2);
end

[M,Index] = min(E);
Da = Dm(Index)
Vtot

c_calc2 = (Atot./(2.*s.*sqrt(pi.*Da*t))).*exp(-((x-Vtot.*t).^2)/(4.*Da*t));
c_calc3 = c_calc2/sum(c_calc2);

figure;
plot(x,cData,'-*',x,c_calc3,'-o');
legend('measured','calculated');
ylabel('c/c_0');
xlabel('x [m]');
```

Appendix 2 Full composition of Boom clay porewater

Element	Mean ^{a)} (ppm)	95 % Confidence Interval		Standard deviation (ppm)
		Lower limit (ppm)	Upper limit (ppm)	
F	3.6	3.3	3.9	0.5
Cl	27	25	29	3
SO ₄ ²⁻	0.2	0	0.6	0.1
Br	0.49	0.45	0.52	0.02
HPO ₄ ²⁻	3.8	3.4	4.3	0.2
HCO ₃ ⁻	828	774	882	34
B	7.5	7.3	7.8	0.3
Na	408	403	413	7
Mg	2.9	2.7	3.1	0.3
Al	0.08	0.05	0.11	0.05
Si ^{b)}	5	0	9	6
K	11	8	13	3
Ca	4.0	3.8	4.3	0.3
Fe	0.9	0.8	1.0	0.2

^{a)} Mean value of following clay waters:

EG/BS.23.10.96;30.10.96;02.09.96;13.06.96;27.06.96;10.05.96;02.04.96;22.11.96;02.12.96;10.01.97;21.01.97

^{b)} Excluding two outliers: mean = 1.9 ppm Si; 95% confidence interval = [1.8; 2.06] ppm Si; standard deviation = 0.2 ppm Si

source: (Dierkx, 1997)

Appendix 3 LabView Script used for monitoring voltage during experiments

```
<VI syntaxVersion=11 LVversion=12008004 revision=35 name="ReadVoltage.vi">
<TITLE><NO_TITLE name="ReadVoltage.vi"></TITLE>
<HELP_PATH></HELP_PATH>
<HELP_TAG></HELP_TAG>
<RTM_PATH type="default"></RTM_PATH>
<DESC></DESC>
<CONTENT>
  <GROUPER>
    <PARTS>
      </PARTS></GROUPER>
    <CONTROL ID=83 type="Cluster" name="error out">
      <DESC><<B>>error in<</B>> can accept error information wired from VIs previously
called. Use this information to decide if any functionality should be bypassed in the event of
errors from other VIs.<LF>
<LF> RightZclick the <<B>>error in<</B>> control on the front panel and select
<<B>>Explain Error<</B>> or <<B>>Explain Warning<</B>> from the shortcut menu for
more information about the error.</DESC>
      <TIP></TIP>
      <PARTS>
        <PART ID=82 order=0 type="Caption"><LABEL><STEXT>error
out</STEXT></LABEL></PART>
      </PARTS>
    <CONTENT>
    (checkmark) to indicate a warning or that no error occurred.<LF>
<LF> RightZclick the <<B>>error in<</B>> control on the front panel and select
<<B>>Explain Error<</B>> or <<B>>Explain Warning<</B>> from the shortcut menu for
more information about the error.</DESC>

<TIP></TIP>
<PARTS>
  <PART ID=22 order=0 type="Boolean
<GROUPER>
  <PARTS>
  </PARTS></GROUPER> <CONTROL ID=79 type="Boolean" name="status">
  <DESC><<B>>status<</B>> is TRUE (X) if an error occurred or FALSE
Text"><MLABEL><STRINGS><STRING></STRING><STRING></STRING><STRING
></STRING><STRING></STRING></S TRINGS></MLABEL></PART>
    <PART ID=82 order=0
type="Caption"><LABEL><STEXT>status</STEXT></LABEL></PART>
<LF> RightZclick the <<B>>error in<</B>> control on the front panel and select
<<B>>Explain Error<</B>> or <<B>>Explain Warning<</B>> from the shortcut menu for
more information about the error.</DESC>
  </PARTS>
</CONTROL>
<CONTROL ID=80 type="Numeric" name="code">
  <DESC><<B>>code<</B>> is the error or warning code.<LF>
type="Caption"><LABEL><STEXT>code</STEXT></LABEL></PART>
```


<TIP></TIP>

<PARTS>

<PART ID=82 order=0

<LF> Right-click the <>error in<> control on the front panel and select <>Explain Error<> or <>Explain Warning<> from the shortcut menu for more information about the error.</DESC>

</PARTS>

</CONTROL>

<CONTROL ID=81 type="String" name="source">

<DESC><>source<> describes the origin of the error or warning.<LF>

type="Text"><LABEL><STEXT></STEXT></LABEL></PART>

<PART

ID=82

order=0

type="Caption"><LABEL><STEXT>source</STEXT></LABEL></PART>

<TIP></TIP>

<PARTS>

<PART ID=11 order=0

</CONTENT> </CONTROL>

</PARTS>

<DEFAULT><SAME_AS_LABEL></DEFAULT> </CONTROL>

<CONTROL ID=94 type="Waveform Chart" name="Waveform Chart">

<DESC></DESC>

<TIP></TIP>

<PARTS>

color=000000>

Chart</STEXT></LABEL></PART>

<PART ID=8022 order=0 type="">

<CONTROL ID=231 type="Tree" >

<DESC></DESC>

<TIP></TIP>

<PARTS>

<GROUPER>

<PARTS>

</PARTS></GROUPER> </PARTS>

</CONTROL> </PART>

</CELL_FONTS> <ROW_HEADER> </ROW_HEADER> <COL_HEADER>

<STRING>Cursors:</STRING> <STRING>X</STRING> <STRING>Y</STRING>

</COL_HEADER> <STRINGS> </STRINGS>

<PRIV>

<CELL_FONTS>

[Z2 Z2] [Z1 Z2]<FONT predef=APPFONT style='B'

```

</PRIV>
<PART ID=82 order=0 type="Caption"><LABEL><STEXT>Waveform
<SCALE_NAMES><STRING>Time</STRING><STRING>Amplitude</STRING></SCALE
LE_NAMES>
</PRIV>
</PARTS>
<PRIV>
<PLOTS><STRING>Plot 0</STRING></PLOTS>
</CONTROL>
<CONTROL ID=79 type="Boolean" name="stop">
color=FF0000<STRINGS><STRING>STOP</STRING><STRING>STOP</STRING><S
TRING>STOP</STRING><STRING>S
TOP</STRING></STRINGS></MLABEL></PART>
</PRIV>
<DESC></DESC>
<TIP></TIP>
<PARTS>
<PART ID=22 order=0 type="Boolean Text"><MLABEL><FONT predef=SYSFONT
<PART ID=82 order=0 type="Caption"><LABEL><STEXT><FONT
predef=DLGFONT color=100000C>stop</STEXT></LABEL></PART>
</PARTS>
</CONTROL>
<CONTROL ID=91 type="Path" name="data file:">
<DESC></DESC>
<TIP></TIP>
<PARTS>
type="Text"><LABEL><STEXT>c:\users\data\test.bin</STEXT></LABEL></PART>
<PART ID=82 order=0 type="Caption"><LABEL><STEXT>data
file:</STEXT></LABEL></PART>
</PARTS>
<PRIV>
<PART ID=8019 order=0 type="Browse Button"> <CONTROL ID=79 type="Boolean"
>
</CONTROL> </PART>
<PART ID=11 order=0
<DESC></DESC> <TIP></TIP> <PARTS> </PARTS>
<PROMPT></PROMPT>
<MTCH_PTN></MTCH_PTN>
<PTN_LBEL></PTN_LBEL>
<STRT_PTH><PATH type="absolute"></PATH></STRT_PTH>
<PTH_BTN_LBL></PTH_BTN_LBL>

</CONTROL>
<CONTROL ID=80 type="Numeric" name="output 1">
1</STEXT></LABEL></PART>

```

```

</PARTS>
</CONTROL> </CONTENT>
<BDCONTENT>

<CONTROL ID=81 type="String Constant" name="format (%.3f)"> <DESC></DESC>
<TIP></TIP>
<PARTS>
  <PART ID=11 order=0
type="Text"><LABEL><STEXT>%.5f</STEXT></LABEL></PART> </PARTS>
  <DEFAULT><SAME_AS_LABEL></DEFAULT>
</CONTROL>
<CONTROL ID=81 type="String Constant" name="delimiter (\t)"> <DESC></DESC>
<TIP></TIP>
<PARTS>
  <PART ID=11 order=0
type="Text"><LABEL><STEXT>,</STEXT></LABEL></PART> </PARTS>
  <DEFAULT><SAME_AS_LABEL></DEFAULT>
</CONTROL>
<CONTROL ID=79 type="False Constant" name="append to file? (new file:F)">
<DESC></DESC>
<TIP></TIP>
<PARTS>
</PARTS>
</CONTROL>
<NODE ID=197 type="PolyVI" subVIName="Write To Spreadsheet File.vi">
  <DESC></DESC>
</NODE>
<NODE ID=47 type="Function" primID=53544446 primName="Format Date/Time String">
  <DESC></DESC>
</NODE>
<NODE ID=47 type="Function" primID=20503253 primName="String To Path">
  <DESC></DESC>
</NODE>
<NODE ID=62 type="Concatenate Strings">
  <DESC></DESC>
</NODE>
<CONTROL ID=81 type="String Constant" >
  <DESC></DESC>
  <TIP></TIP>
  <PARTS>
    <PART ID=11 order=0
type="Text"><LABEL><STEXT></STEXT></LABEL></PART>
    </PARTS>
    <DEFAULT><STRING>d:\</STRING></DEFAULT>
  </CONTROL>
<CONTROL ID=81 type="String Constant" >
  <DESC></DESC>
  <TIP></TIP>
  <PARTS>

```

```

    <PART ID=11 order=0
type="Text"><LABEL><STEXT>.csv</STEXT></LABEL></PART> </PARTS>
  <DEFAULT><SAME_AS_LABEL></DEFAULT>
</CONTROL>
<NODE ID=62 type="Concatenate Strings">
  <DESC></DESC>
</NODE>
<CONTROL ID=81 type="String Constant" name="time format string (%c)">
<DESC></DESC>
<TIP></TIP>
<PARTS>
  <PART ID=11 order=0 type="Text"><LABEL><STEXT></STEXT></LABEL></PART>
</PARTS>
<DEFAULT><STRING>%y%m%d%H%M</STRING></DEFAULT>
<DEFAULT>
  <PATH type="absolute">c<SEP>users<SEP>data<SEP>test.bin</PATH> </DEFAULT>
<DESC></DESC>
<TIP></TIP>
<PARTS>
  <PART ID=82 order=0 type="Caption"><LABEL><STEXT>output
</CONTROL>
  <CONTROL ID=85 type="VISA resource name" name="VISA resource name">
    <DESC></DESC>
    <TIP></TIP>
  <PARTS>
</PARTS>
</CONTROL>
  <PART ID=8017 order=0 type="I/O Name Display">
    <CONTROL ID=148 type="VISA USB Control Out" >
</CONTROL> </PART>
  <NODE ID=33 type="While Loop">
    <DESC></DESC>
    <BDCONTENT>
type="Text"><LABEL><STEXT>%f</STEXT></LABEL></PART>
primName="Equal?">

```

```

  Read STB">
  FETCH?</STEXT></LABEL></PART>
<DESC></DESC> <TIP></TIP> <PARTS> </PARTS>
<CONTROL ID=80 type="Numeric Constant" name="milliseconds to wait">
<DESC></DESC>
  <TIP></TIP>
  <PARTS>
</PARTS>
</CONTROL> <NODE ID=47 type="Function" primID=54494157 primName="Wait
(ms)"> <DESC></DESC>
</NODE> <CONTROL ID=81 type="String Constant" name="format string">
  <DESC></DESC>
  <TIP></TIP>

```

```

<PARTS>
  <PART ID=11 order=0
</PARTS>
<DEFAULT><SAME_AS_LABEL></DEFAULT> </CONTROL> <NODE ID=146
type="Scan From String">
  <DESC></DESC>
</NODE>
<NODE ID=33 type="While Loop">
  <DESC></DESC>
  <BDCONTENT>

<CONTROL ID=80 type="Numeric Constant" name="y"> <DESC></DESC>
  <TIP></TIP>
  <PARTS>
  </PARTS>
</CONTROL> <NODE ID=47 type="Function" primID=20205145
  <DESC></DESC>
</NODE> <NODE ID=47 type="Function" primID=42545356 primName="VISA

</BDCONTENT>
</NODE> <CONTROL ID=81 type="String Constant" name="write buffer">
  <DESC></DESC> </NODE>
<DESC></DESC>
<TIP></TIP>
<PARTS>
  <PART ID=11 order=0 type="Text"><LABEL><STEXT>INIT<LF>
  </PARTS>
  <DEFAULT><SAME_AS_LABEL></DEFAULT>
</CONTROL> <NODE ID=47 type="Function" primID=54525756 primName="VISA
Write"> <DESC></DESC>
</NODE>
<CONTROL ID=80 type="Numeric Constant" name="byte count">
<DESC></DESC> <TIP></TIP> <PARTS>
</BDCONTENT>
</NODE>
  <NODE ID=33 type="While Loop">
    <DESC></DESC>
    <BDCONTENT>
  </BDCONTENT>
</NODE>
  </PARTS>
</CONTROL> <NODE ID=47 type="Function" primID=20445256 primName="VISA
Read"> <DESC></DESC>
</NODE>
<CONTROL ID=80 type="Numeric Constant" name="y"> <DESC></DESC>
  <TIP></TIP>
  <PARTS>
  </PARTS>

```

```

</CONTROL> <NODE ID=47 type="Function" primID=20205145 primName="Equal?">
  <DESC></DESC>
</NODE> <NODE ID=47 type="Function" primID=42545356 primName="VISA Read
STB"> <DESC></DESC>
</NODE>
  <CONTROL ID=81 type="String Constant" name="write buffer">
CONF:VOLT:DC<LF> TRIG:SOUR IMM<LF> *OPC</STRING></DEFAULT>
  </CONTROL>
<DESC></DESC>
<TIP></TIP>
<PARTS>
  <PART ID=11 order=0 type="Text"><LABEL><STEXT></STEXT></LABEL></PART>
</PARTS>
<DEFAULT><STRING>*ESE 1<LF>
  <NODE ID=47 type="Function" primID=54525756 primName="VISA Write">
  <DESC></DESC>
  </NODE>
  <CONTROL ID=81 type="String Constant" name="write buffer">
</CONTROL>
  <NODE ID=47 type="Function" primID=534C4356 primName="VISA Close">
  <DESC></DESC>
<DESC></DESC>
<TIP></TIP>
<PARTS>
  <PART ID=11 order=0 type="Text"><LABEL><STEXT></STEXT></LABEL></PART>
</PARTS>
<DEFAULT><STRING>*CLS</STRING></DEFAULT>
  </NODE>
  <NODE ID=47 type="Function" primID=54525756 primName="VISA Write">
  <DESC></DESC>
  </NODE>
  <NODE ID=47 type="Function" primID=524C4356 primName="VISA Clear">
  <DESC></DESC>
  </NODE>
</BDCONTENT>
</VI>

```